Carbohydrate Polymers 113 (2014) 231–239

Contents lists available at ScienceDirect

Carbohydrate Polymers

journal homepage: www.elsevier.com/locate/carbpol

Electrospinning of chitosan/sericin/PVA nanofibers incorporated with in situ synthesis of nano silver

Elmira Hadipour-Goudarzi, Majid Montazer*, Masoud Latifi, Ali Akbar Ghare Aghaji

Department of Textile Engineering, Modern Fibrous Structures & Environmental Enhancement (FFSEE), Amirkabir University of Technology, Tehran, Iran

ARTICLE INFO

Article history:
Received 27 March 2014
Received in revised form 18 June 2014
Accepted 20 June 2014
Available online 11 July 2014

Keywords:
Electrospinning
Chitosan
Sericin
PVA
Nanofibers
In situ synthesis
Nano silver

ABSTRACT

Here, chitosan/sericin/poly(vinyl alcohol) as a biodegradable nanofibrous membrane was prepared through electrospinning with and without silver nitrate. The influences of spinning conditions including volume ratio of chitosan and sericin, voltage and spinning distance at constant feed rate on the fiber morphology and size distribution were examined by SEM and *Image J* software. The FT-IR spectrum and EDAX were used to indicate the chemical structure of nanofibrous membrane. In addition, the effect of $AgNO_3$ on the nanofibers diameter and its antibacterial activity was investigated. The optimum conditions obtained with chitosan:sericin (50:50, v/v), 22 kV voltage, 10 cm spinning distance at 0.25 mL/h feed rate to prepare nanofibers with small diameter and narrow size distribution without beads. The mean diameter of nanofibers was about 180 nm while introducing $AgNO_3$ led to smaller nanofibers diameter about 95 nm. Moreover, the presence of $AgNO_3$ produced an excellent antibacterial activity against *Escherchia coli*.

1. Introduction

Electrospinning is one of the conventional, simple and efficient method to produce nanofibers from wide variety of polymers in different forms (Bhardwaj & Kundu, 2010; Khajavi & Abbasipour, 2012; Ramakrishna, Fujihara, Teo, Lim, & Ma, 2005). Nanofibers have unique properties such as high surface area to volume ratio and high porosity with various pore size (Bhardwaj & Kundu, 2010; Khajavi & Abbasipour, 2012). They are used in diverse fields including filtration (Biorge et al., 2009; Muzzarelli, Weckx, & Filippini, 1989), drug delivery (Sill & Recum, 2008), wound dressing (Jin et al., 2013), cell culture, tissue engineering and many others (Celebioglu et al., 2014; Mottaghitlab et al., 2011; Muzzarelli, Greco, Busilacchi, Sollazzo, & Gigante, 2012; Muzzarelli, 2009, 2011a,b). Also, different natural polymers have been electrospun for biomedical applications such as collagen (Su Rho et al., 2006), chitin/chitosan (Elsabee, Naguib, & Elsayed Morsi, 2012), silk fibroin (Min et al., 2004) and poly(L-lactic acid) (Chen, Tseng, Delimartin, Lee, & Ho, 2008).

Chitosan as a linear polysaccharide is produced from deacetylation of chitin (Domard, 2011). Chitosan has good biocompatibility, biodegradability, antimicrobial activity, wound healing property and antitumor effect (Ravi Kumar, 2000). This has also potential in varies applications including filtration, removal of uranium, drug-delivery, wound dressing, cell culture, tissue engineering, photography, cosmetic, ophthalmology and solid-state batteries (Aroon, Ismail, Montazer-Rahmati, & Matsura, 2010; Domard, 2011; Muzzarelli et al., 1989; Muzzarelli, 1985, 2011a,b; Ravi Kumar, 2000). Moreover, the solubility of chitosan in common organic solvent is poor due to the rigid D-glucosamine repeat unit, high crystalline and ability to hydrogen bonding making difficult to electrospin (Elsabee et al., 2012). Some ways such as electrospinning of chitosan derivatives, chitosan blends and quaternized chitosan have been approved to improve electrospinning (Elsabee et al., 2012). Further, there are many reports on electrospinning of chitosan such as chitosan dissolved in concentrated acetic acid (Geng, Kwon, & Jang, 2005), trifluoroacetic acid (TFA)/dichloromethane (DCM) (Sencadas et al., 2012), chitosan blended with poly(ethylene oxide) (Dilamian, Montazer, & Masoumi, 2013) gelatin (Zhuang, Cheng, Kang, & Xu, 2010) silk fibroin (Park, Jong, Dong, & Hudson, 2004) and poly(vinyl alcohol) (PVA) (Abdelgawad, Hudson, & Rojas, 2014; Jia et al., 2007; Mottaghitlab et al., 2011). Furthermore, adding nano particles such as nano silver and nano ZnO to chitosan solution have been utilized to improve special characteristic such as antimicrobial

* Corresponding author at: Textile Department, Modern Fibrous Structures & Environmental Enhancement (FFSEE), Amirkabir University of Technology, Hafez Avenue, Tehran, Iran. Tel.: +98 2164542657; fax: +98 2166400245.
E-mail address: tex5mm@aut.ac.ir (M. Montazer).

http://dx.doi.org/10.1016/j.carbpol.2014.06.082
0144-8617/

activity (Abdelgawad et al., 2014; Wang, Zhang, Zhang, & Li, 2012; Zhuang et al., 2010). There are also many reports regarding in situ synthesis of nano silver on various materials such as chitosan to improve their antibacterial activity (Abdelgawad et al., 2014; Celebioglu et al., 2014; Montazer, Shamei, & Alimohammadi, 2012; Montazer, Alimohammadi, Shamei, & Rahimi, 2012; Terada, Sasaki, Yanagihara, & Yamada, 2005; Zhuang et al., 2010).

Silk is a natural protein, mainly envelops sericin and fibroin (Zhang, 2002). Sericin consists of many amino acids which mostly having strong polar side groups such as hydroxyl, carboxyl and amine (Kim, 2007; Zhang, 2002). It has useful properties such as biocompatibility, biodegradability, antibacterial activity, UV resistant, oxidation resistant, cell proliferation and mineral absorption with easily absorption and desorption moisture (Dash, Mandal, & Kundu, 2009; Doakhan, Montazer, Rashidi, Moniri, & Moghadam, 2013; Terada et al., 2005; Zhang, 2002). Therefore, it has been incorporated to practical use in biodegradable and membrane materials, functional and medical biomaterials and functional fiber fabrics (Zhang, 2002), as well as in skin care, medical and food industries (Dash et al., 2009), cell culture (Doakhan et al., 2013; Kundu & Kundu, 2012), dermal reconstruction (Gimenes, Liu, & Feng, 2007) and tissue engineering (Aramwit, Siritientong, Kanokpanont, & Srichana, 2010; Dash et al., 2009).

There are many reports in film formation of sericin (Kim, 2007; Gimenes et al., 2007; Srihanam, Simcheur, & Srisuwan, 2009). Moreover there are a few studies about preparation of sericin nanofibers through electrospinning. Sericin solution dissolved in TFA was successfully electrospun to nanofibers (Zhang, Rahman Khan, Yamamoto, Tsukada, & Morikawa, 2012), as well as silk sericin/silk fibroin mixed solution dissolved in TFA (Zhang et al., 2011). Furthermore, fibroin/sericin core-shell nanofibers were prepared with coaxial electrospinning of fibroin/sericin aqueous solution (Hang, Zhang, Jin, Shao, & Hu, 2012).

In this study, the nanofibrous mat of chitosan(Cs)/sericin (SS)/PVA composite has been spun through electrospinning. The effect of different electrospinning conditions on the morphology and diameter of nanofibers was investigated. FTIR spectrum and EDAX pattern were used to determine the chemical structure of the nanofibers. Furthermore the effect of $AgNO_3$ was investigated on nanofibers diameter and its antibacterial activity against *Escherichia coli*.

2. Experimental

2.1. Materials

Medium molecular weight chitosan with degree of deacetylation (DD) 75–85% was purchased from Aldrich Co., USA. Silk sericin (M_w = 500–1000, pH = 4.5–6.5) was prepared from Huzhou, China. Poly(vinyl alcohol) (PVA) (M_w = 72,000) and acetic acid were supplied from Merck Co, Germany. Silver nitrate was supplied from Aldrich Co, USA. The Gram-negative bacteria *E. coli* (ATCC 25922) were used.

2.2. Electrospinning solutions preparation

PVA and sericin solutions 10 wt% were separately prepared by dispersion of PVA and sericin in distilled water and then stirred for 24 h at 50 °C for PVA and room temperature for sericin. Similarly, chitosan solution 3 wt% was prepared in 90% acetic acid for 48 h at room temperature. Chitosan and sericin solutions were mixed at different volume ratio (Cs:SS) including 30:70, 50:50 and 70:30 and then stirred for 24 h at room temperature. Each prepared Cs/SS solutions were mixed with PVA solution 10 wt% at constant volume ratio 50:50. Therefore, three solutions including Cs:SS:PVA (15:35:50), Cs:SS:PVA (25:25:50) and Cs:SS:PVA (35:15:50) were prepared before electrospinning.

2.3. Electrospinning

The prepared solutions were supplied into a 5 mL syringe with a metal capillary needle (inner diameter = 0.5 mm). The electrospinning were performed at room temperature and the solutions were injected from the syringe pump with feed rate of 0.25 mL/h. The electrospun nanofibers were assembled on a rotated drum (coated with aluminum foil) as a collector which was placed at 10 cm or 15 cm from the needle tip and the high voltage was applied at 17, 22 and 27 kV.

2.4. Morphology of electrospun nanofibers

The surface morphology and diameter of the electrospun nanofibers were observed with a scanning electron microscope (SEM; *Philips XL30*, Netherlands). A small section of aluminum foil which coated with electrospun nanofibers was cut and sputter coated with gold/palladium for 160 s (sputter coater: *Emitech SC7620*) to prevent charging. In order to determine average fiber diameters size and distribution of each electrospun nanofibrous mat, 30 fibers were randomly selected from each SEM images and the diameter of 2 points along each fiber (total 60 points) was measured by using image analysis software *Image-J* (NIH, USA).

2.5. Energy dispersed X-ray spectroscopy

EDAX (*Philips XL30*, Netherlands) was used to indicate the element combination or part of sample. EDAX does not use alone, but it is used as a part of SEM.

2.6. Fourier transform infrared spectroscopy

The chemical structure of nanofibrous mats was studied with FTIR spectra. All spectrum were taken at room temperature on a spectrometer (Thermo Nicolet, *Nexus670*, USA) with spectral range of 4000–500 cm^{-1} and 4.0 cm^{-1} resolution. In order to determine the FTIR spectrum and collected data, *OMNIC* software was used. Spectra were performed for PVA, Cs and SS powders and Cs/SS/PVA nanofibrous mat.

2.7. Antibacterial activity test

The antibacterial test against Gram negative bacteria, *E. coli* (ATCC 25922) was carried out by standard quantitative test method (AATCC 100). Circular pieces (5 cm diameter, 0.5 cm thickness) were cut from nanofibrous mats and placed in polystyrene tubes and sterilized in incubator for 20 min. *E. coli* was grown in nutrient broth at 37 °C for 18 h, then bacterial cells were collected by centrifuge at 4 °C (8000 rpm,10 min). Bacterial pellet was washed with sterile phosphate buffered saline (PBS; pH = 7.2) three times to remove any source of nutrition. Bacterial cells were re-suspended in sterile PBS to an optical density of 0.1 at 620 nm which is equivalent to 1.5×10^8 CFU mL^{-1}; then diluted to a suspension containing 10^7 CFU mL^{-1}. Each sterilized sample was inoculated with 0.1 mL bacterial suspension and incubated overnight at room temperature. After incubation period, 20 mL sterile PBS was added to each tube and vigorously vortexed for 3 min. The serial-dilutions from each sample were prepared by 1:10 and then 0.1 mL of proper dilutions was spread on nutrient agar plates. Cultures were incubated at 37 °C for 18 h and then concentration of *E. coli* for each sample was calculated (CFU mL^{-1}). PVA nanofibrous mat was considered as negative control which no antibacterial activity was expected and

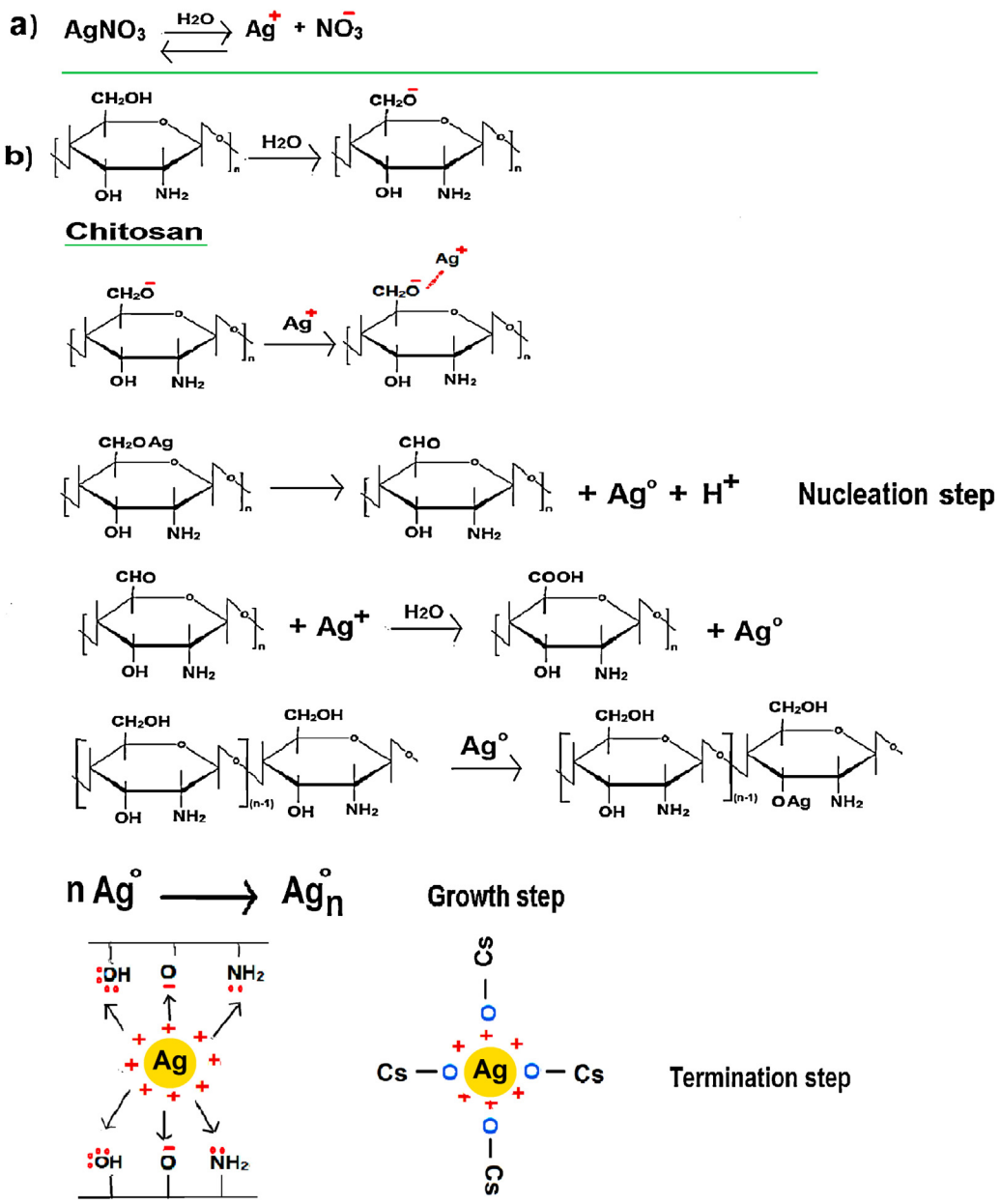

Fig. 1. Mechanism reaction of (a) $AgNO_3$ in water and (b) synthesis of Ag with Cs.

Cs/SS/PVA and Cs/SS/PVA/$AgNO_3$ nanofibrous mats were tested. The antibacterial activity was calculated using (Eq. (1)).

$$R = \frac{100(B - A)}{B} \quad (1)$$

where R is the bacteria reduction percentage, A is the number of remained bacteria after 24 h and B is the number of bacteria before incubation the plates.

3. Results and discussion

3.1. Intermolecular interactions between chitosan, sericin, PVA and $AgNO_3$

The chemical structure of chitosan, sericin and PVA consist of functional groups including (—OH and $—NH_2$), (—OH, $—NH_2$ and —COOH) and (—OH) respectively indicate good potential for interaction with each others. There are also intermolecular interactions between Cs and SS (Srihanam et al., 2009) SS and PVA (Aramwit et al., 2010; Dash et al., 2009; Kim, 2007; Kundu & Kundu, 2012) as well as Cs and PVA through hydrogen bonding (Abdelgawad et al., 2014; Jia et al., 2007). All these three compounds have electron donor groups capable to reduce $AgNO_3$ to Ag°. Oxygen-rich polysaccharide chitosan interacts with electropositive metal cation, Ag^+ reducing to Ag° (Zhuang et al., 2010). The reaction of hydroxyl groups of chitosan with electropositive Ag^+ in aqueous media is shown in Fig. 1(b). Furthermore, PVA was used as a reducing agent to synthesis silver nanoparticles (Celebioglu et al., 2014). The reaction of hydroxyl groups of PVA in water with Ag^+ is demonstrated in Fig. 2. In addition, sericin was also reduced Ag^+ to Ag° (Terada et al., 2005). The interactions between functional groups of sericin dissolved in water and Ag^+ were shown in Fig. 3. Three reduction steps of Ag^+ to silver nanoparticles including nucleation, growth and termination were schematically indicated

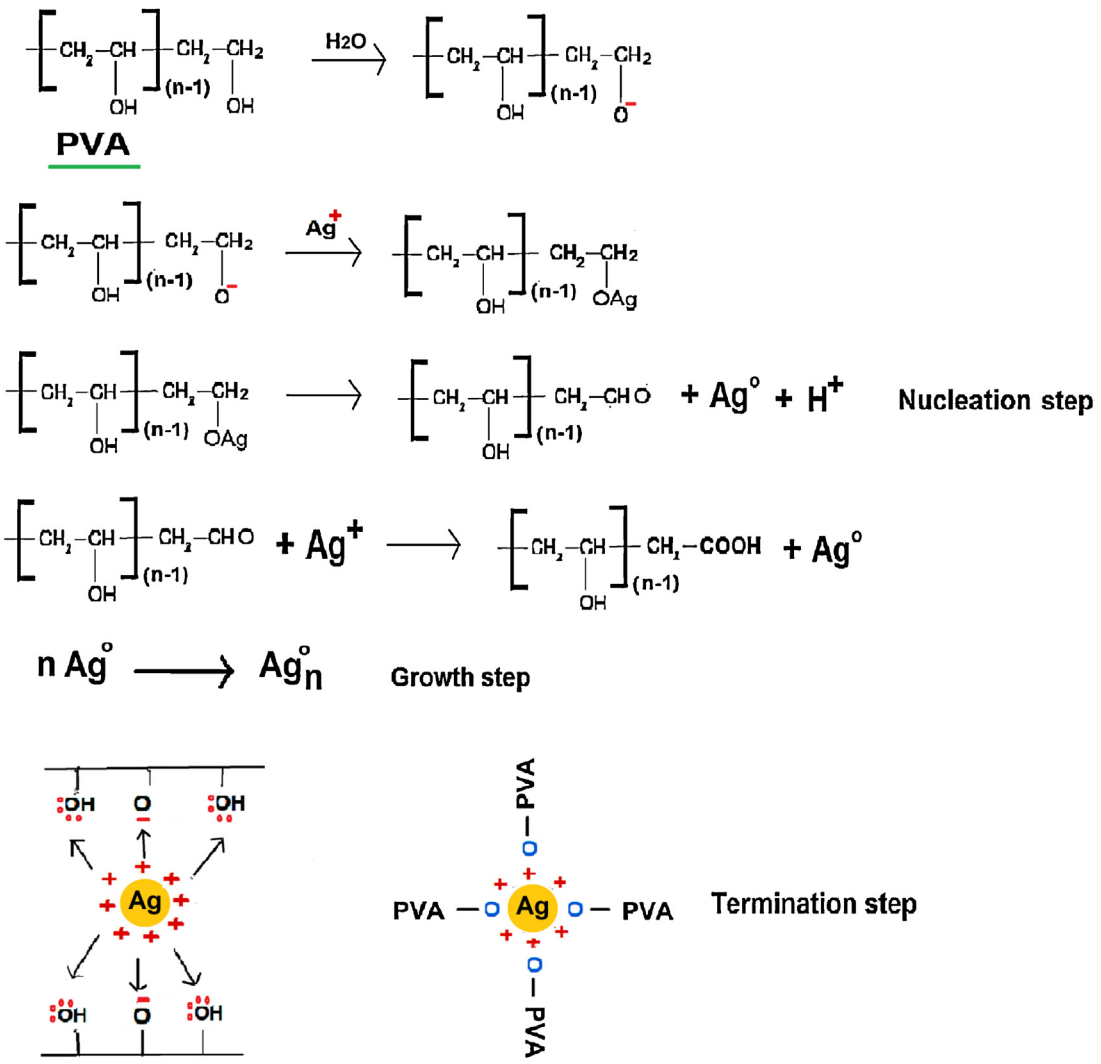

Fig. 2. Mechanism reaction of synthesis of Ag with PVA.

in Figs. 1–3. The possible interactions between Cs, SS and PVA with Ag^+ that was leading to synthesis Ag° are also shown in Fig. 4.

3.2. Morphology of electrospun nanofibers

The morphology and diameter of electrospun nanofibers are determined through SEM images and *Image J* software. The affecting parameters on electrospinning and production of nanofibers have been broadly classified into polymer solution, processing conditions and ambient conditions (Ramakrishna et al., 2005). In order to prepare Cs/SS/PVA electrospun nanofibers in optimum conditions; the effect of variable parameters including volume ratio of Cs:SS, voltage and spinning distance at constant feed rate were examined on the fiber morphology and size distribution.

3.2.1. Effect of volume ratio of Cs:SS

The SEM images and diameter distribution histograms of Cs/SS/PVA nanofibers with different volume ratios at three voltages (17, 22 and 27 kV) and two spinning distances (10 and 15 cm) at constant feed rate 0.25 mL/h are demonstrated in Fig. 5.

The polymer solution properties have the most significant influence on the nanofibers morphology. The viscosity of the solution determines the extent of the solution stretch (Ramakrishna et al., 2005). Chitosan with a cationic charge produces a high viscose solution and blending with nonionic polymers helps electrospinning (Elsabee et al., 2012). Therefore Cs/SS solutions are prepared at different volume ratios and then mixed with PVA solution (volume ratio 50:50). The effect of increasing percentage of chitosan in the solutions is investigated on the morphology and diameter of the electrospun nanofibers. The SEM images of Cs:SS:PVA (15:35:50) nanofibers in various processing conditions indicated plenty beads in their structure while decreased for two other ratios. Furthermore, the Cs:SS:PVA (25:25:50) nanofibers showed smaller nanofibrous mean diameter than Cs:SS:PVA (35:15:50) nanofibers whereas the diameter distributions were more narrower. This can be due to the viscosity changes of various volume ratios. The higher solution viscosity leads to more polymer chain entanglement and higher solution resistance against stretching (Ramakrishna et al., 2005). Therefore higher solution viscosity leads to the larger nanofibers diameter and lower beads formation along the nanofibers in their structures. On these bases, the Cs/SS/PVA solution with 50:50 ratio of Cs:SS was the most suitable solution for preparation bead free nanofibrous with narrow and uniform diameter.

3.2.2. Effect of spinning distance

To compare the effect of spinning distance on the morphologhy and diameter of nanofibers, the Cs/SS/PVA solution was electrospun

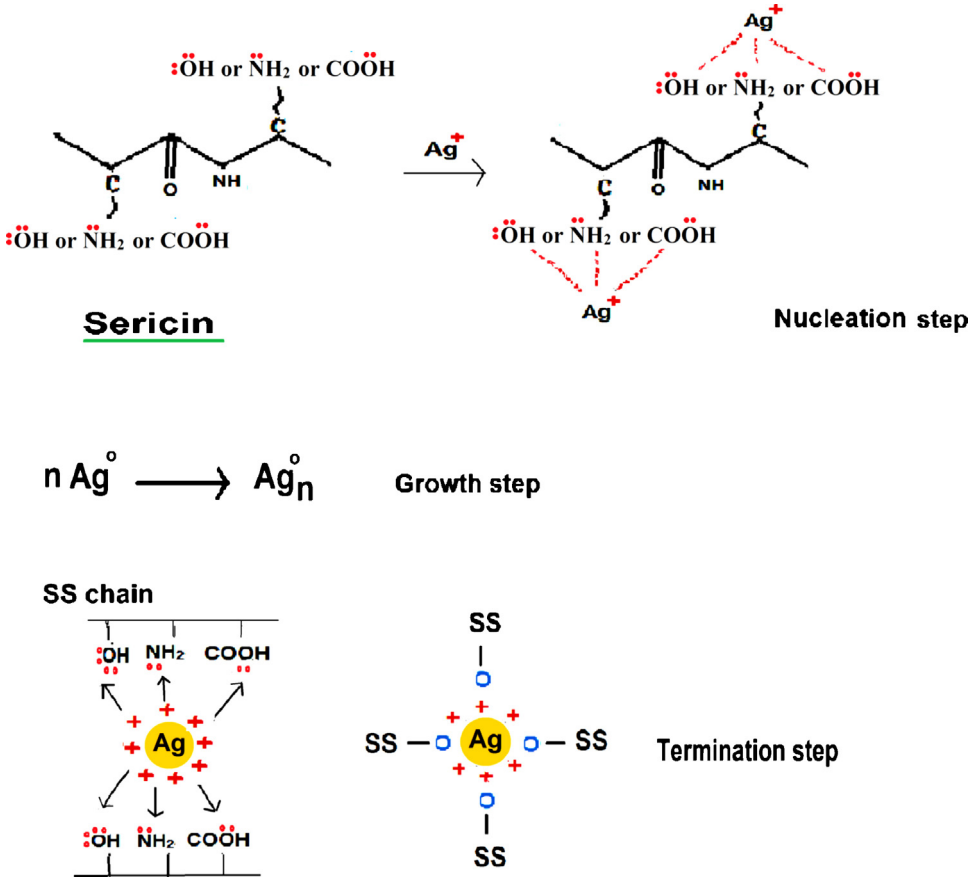

Fig. 3. Mechanism reaction of synthesis of Ag with SS.

at two different distances (10 and 15 cm). The SEM images of Cs:SS:PVA (25:25:50) at constant voltage of 22 kV, feed rate of 0.25 mL/h and distance of 10 cm (sample e) and 15 cm (sample n) are shown in Fig. 5. The diameter distribution of nanofibers at distance of 10 cm is narrower than 15 cm. The number of beads is also lower. Moreover, the mean nanofibers diameter is larger at 10 cm as the longer distance lead to longer flight time needed to stretch solution before deposition on the collector. Thus the average diameter of nanofibers decreased. Moreover, longer distance leads to the higher instability of the jet increasing the diameter distribution and number of beads (Ramakrishna et al., 2005).

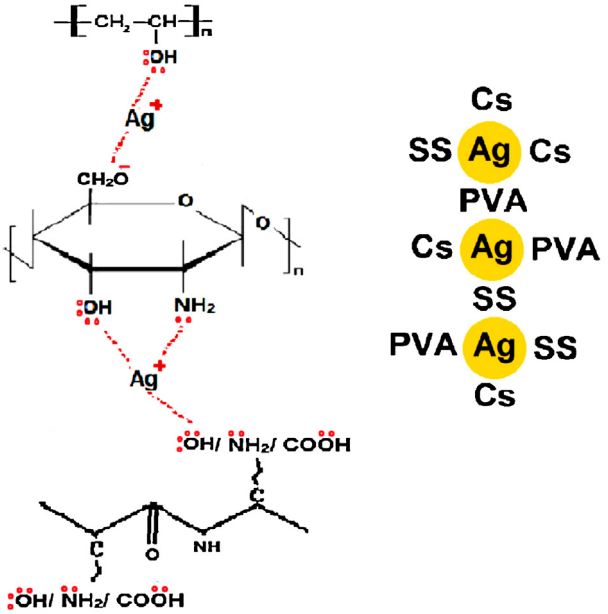

Fig. 4. Mechanism reaction of synthesis of Ag with Cs/SS/PVA.

3.2.3. *Effect of applied voltage*

The SEM images and diameter distribution histograms of Cs:SS:PVA (25:25:50) nanofibrous mat at 10 cm, 0.25 mL/h and varied voltages including 17 kV (sample b), 22 kV (sample e) and 27 kV (sample h) are shown in Fig. 5. The mean diameter and its distribution of nanofibers decrease with increasing voltages (Geng et al., 2005; Ramakrishna et al., 2005; Sencadas et al., 2012; Zhang et al., 2012). Higher voltage leads to more stretching of the solution because of more columbic forces in the jet decreasing the fiber diameter (Ramakrishna et al., 2005; Sencadas et al., 2012).

The mean diameter and its distribution of nanofibers are lowest at 27 kV moreover, some beads are observed among nanofibers at 27 kV. In addition, the diameter distribution diagram at 22 kV is closer to normal diagram than 27 kV. Therefore, 22 kV was chosen to produce more suitable nanofibers.

3.2.4. *Effect of $AgNO_3$ on Cs/SS/PVA nanofibers diameter*

The Cs/SS/PVA nanofibers in presence of $AgNO_3$ (1 wt% Cs/SS/PVA solution) (Cs/SS/PVA/$AgNO_3$) was electrospun in optimum conditions obtained from electrospinning of nanofibrous mat without silver nitrate. The SEM images of Cs/SS/PVA nanofibers with and without $AgNO_3$ are shown in Fig. 6(a) and (b). The mean diameter of Cs/SS/PVA/$AgNO_3$ is half of Cs/SS/PVA

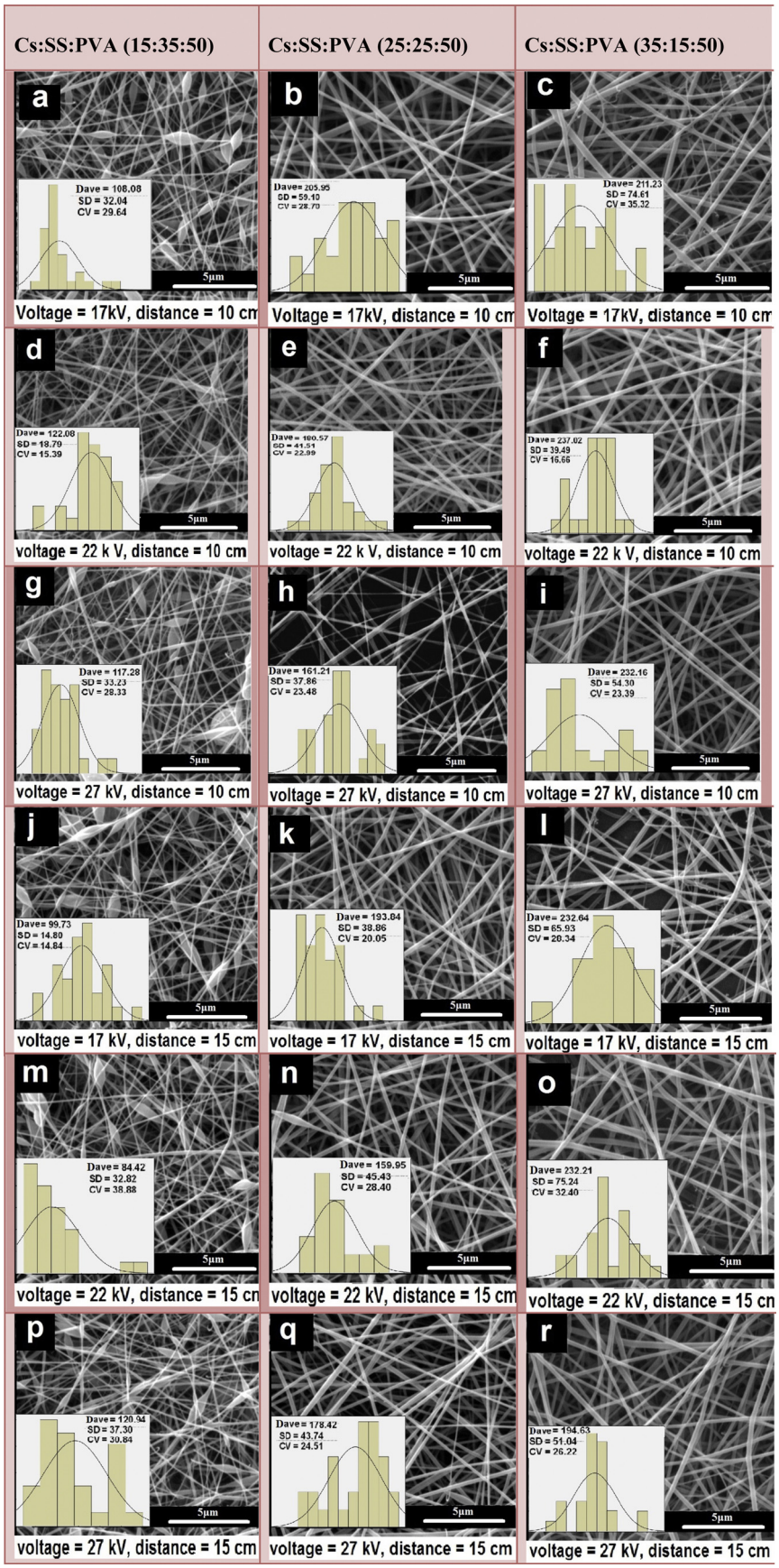

Fig. 5. SEM images and diameter distribution histograms of Cs/SS/PVA nanofibers with different volume ratios at three voltages (17 kV, 22 kV and 27 kV) and two spinning distance (10 cm and 15 cm) at constant feed rate 0.25 mL/h.

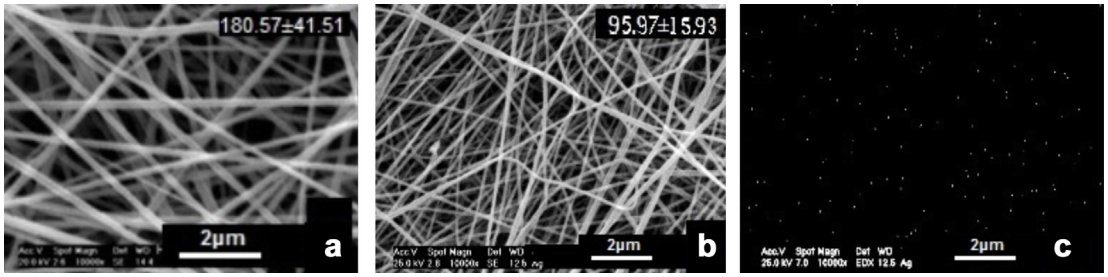

Fig. 6. SEM images of Cs:SS:PVA (25:25:50) nanofibrous mats produced at 10 cm distance, 22 kV voltage and 0.25 mL/h feed rate. (a) Without $AgNO_3$, (b) with $AgNO_3$ and (c) EDAX pattern of nano silvers.

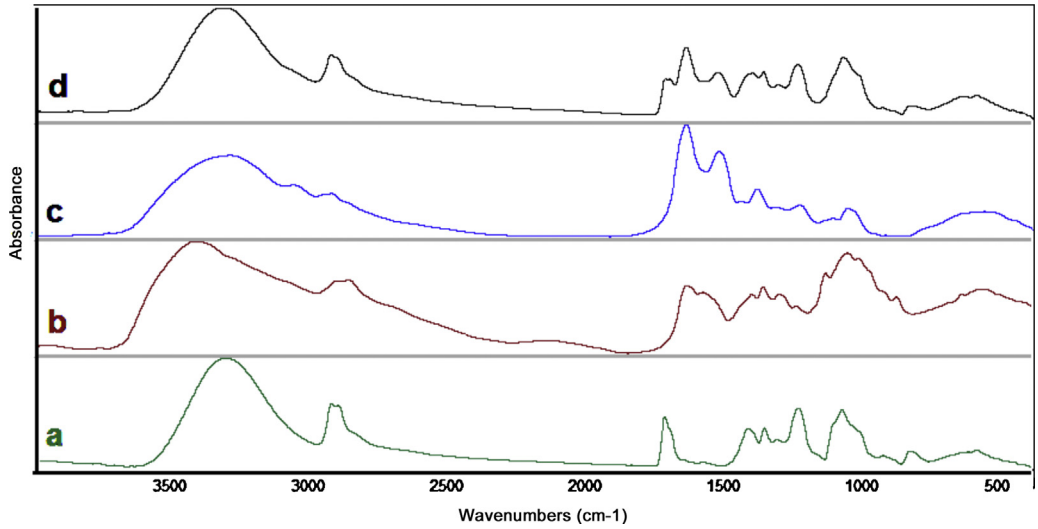

Fig. 7. FTIR spectrums of (a) PVA powder, (b) Cs powder, (c) SS powder and (d) Cs/SS/PVA nanofibrous mat.

nanofibers. Therefore, introducing $AgNO_3$ in electrospinnning solution decreases the mean diameter of nanofibers (Abdelgawad et al., 2014). $AgNO_3$ in the spinning solution leads to the more charge density in the solution increasing the columbic forces and stretching of the solution similar to increasing voltage.

3.3. EDAX spectroscopy

The EDAX pattern of Cs/SS/PVA/$AgNO_3$ nanofibrous mat is shown in Fig. 6(c). The white points on the nanofibers exhibit the nano silvers which well distributed into nanofibrous mat. Therefore, in situ reduction of $AgNO_3$ to Ag nanoparticles was carried out with chitosan, sericin and PVA (Celebioglu et al., 2014; Terada et al., 2005; Zhuang et al., 2010).

3.4. FTIR spectroscopy

FTIR spectrum of Cs, SS and PVA powders and Cs/SS/PVA nanofibrous mat are shown in (Fig. 7). The FTIR spectra of PVA exhibits peaks at 3319 cm^{-1}, 2937 cm^{-1}, 1431 cm^{-1} and 1093 cm^{-1} which are attributed to OH, CH, CHOH and CO groups respectively (Jia et al., 2007). Chitosan powder shows absorption peak at 3427 cm^{-1} assigns to N—H, O—H stretching vibration and inter molecular hydrogen bonding of chitosan backbone (Dilamian et al., 2013; Jia et al., 2007). The feature peaks at 1656 cm^{-1} and 1590 cm^{-1} are assigned to amide I and amide II, respectively (Dilamian et al., 2013; Jia et al., 2007). Furthermore, the peaks at 1378 cm^{-1} and 1256 cm^{-1} are related to C—H and C—O bonds respectively (Dilamian et al., 2013; Jia et al., 2007; Srihanam et al., 2009). The Sericin powder shows absorption peaks at 1655 cm^{-1}, 1538 cm^{-1}

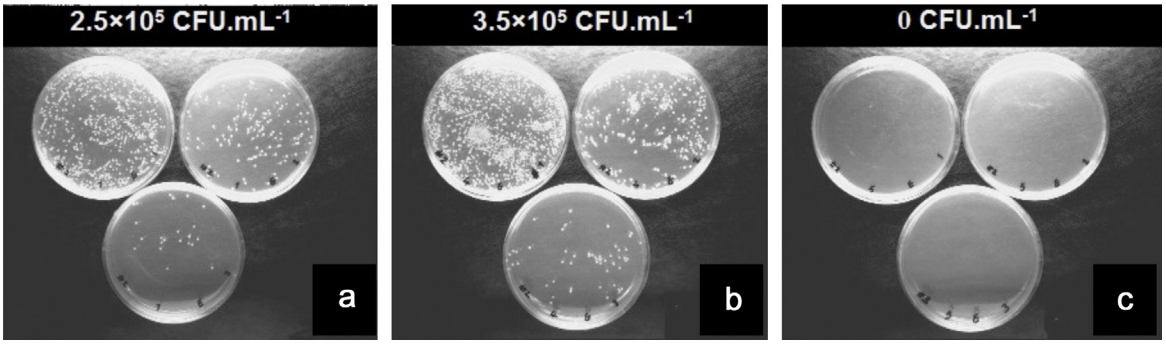

Fig. 8. Antibacterial activity of nanofibrous mats against *E. coli*. (a) PVA: 2.5 × 10^5 CFU mL^{-1}, (b) Cs/SS/PVA: 3.5 × 10^5 CFU mL^{-1} and (c) Cs/SS/PVA/$AgNO_3$: 0 CFU mL^{-1}.

and 1245 cm^{-1} which are attributed to amide I, amide II and amide III groups respectively (Aramwit et al., 2010; Srihanam et al., 2009; Zhang et al., 2011, 2012). In addition, the peak at 2936 cm^{-1} is assigned to C—H bonds and peak at 3302 cm^{-1} related to NH and OH groups (Aramwit et al., 2010; Doakhan et al., 2013; Zhang et al., 2011, 2012). The FTIR spectra of Cs/SS/PVA nanofibrous mat exhibits peak at 3384 cm^{-1} concerned with O—H and N—H stretching vibration and inter hydrogen bonding and peaks at 2938 cm^{-1}, 1656 cm^{-1} and 1541 cm^{-1} are assigned to C—H, C=O (amide I) and N—H (amide II) bonds. Therefore the Cs/SS/PVA nanofibrous mat composed of all Cs, SS and PVA compounds (Srihanam et al., 2009).

3.5. Antibacterial activity test

The antibacterial activity of Cs/SS/PVA nanofibrous mats with and without $AgNO_3$ was evaluated via quantitative test against a Gram-negative bacterium, *E. coli* (ATCC 25922). Fig. 8 shows the growth rate of *E. coli* after being exposed and incubated with PVA (2.5×10^5 CFU mL^{-1}), Cs/SS/PVA (3.5×10^5 CFU mL^{-1}) and Cs/SS/PVA/$AgNO_3$ (0 CFU mL^{-1}). Considering PVA nanofibrous mat as non-antibacterial control; the number of recovered bacterial colonies from Cs/SS/PVA nanofibrous mats shows no antibacterial activity against *E. coli* (0%). Cs/SS/PVA/$AgNO_3$ nanofibrous mat completely killed the bacteria showed 100% antibacterial activity against *E. coli*. Many researchers reported the antimicrobial activity of $AgNO_3$ (Abdelgawad et al., 2014) due to attaching the nano silver (achieved from in situ reduction of silver salt) to the bacteria cell wall and disturbing wall permeability and cellular respiration.

4. Conclusion

The Cs/SS/PVA nanofibers incorporated with in situ synthesis of nano silver were successfully produced through electrospinning. The optimum conditions of volume ratio of Cs:SS (50:50), spinning distance 10 cm and applied voltage 22 kV at feed rate 0.25 mL/h obtained for preparation of Cs/SS/PVA nanofibers with mean diameter about 180 nm. Longer distance leads to the wider diameter distribution and more beads formation in the nanofibrous mat as well as smaller mean diameter. Also, higher voltage leads to lower nanofiber diameter and more beads formation among the nanofibers. Introducing $AgNO_3$ not only produces excellent antibacterial activity, also decreases the Cs/SS/PVA/$AgNO_3$ nanofiber diameter to about 95 nm. Consequently, the Cs/SS/PVA/$AgNO_3$ nanofibrous mat has a great potential for tissue engineering because of its unique components and structure. We purpose to investigate the effect of chitosan and sericin on ability of cell culture in Cs/SS/PVA nanofibrous mat in the future.

References

Abdelgawad, A. M., Hudson, S. M., & Rojas, O. J. (2014). Antimicrobial wound dressing nanofiber mats from multicomponent (chitosan/silver-NPs/polyvinyl alcohol) systems. *Journal of Biological Macromolecules*, *100*, 166–178.

Aramwit, P., Siritientong, T., Kanokpanont, S., & Srichana, T. (2010). Formulation and characterization of silk sericin–PVA scaffold crosslinked with genipin. *Journal of Biological Macromolecules*, *47*, 668–675.

Aroon, M. A., Ismail, A. F., Montazer-Rahmati, M. M., & Matsura, T. (2010). Effect of chitosan as a functionalization agent on the performance and separation properties of polyimide/multi-walled carbon nanotubes mixed matrix flat sheet membranes. *Journal of Membrane Science*, *364*, 309–317.

Bhardwaj, N., & Kundu, S. C. (2010). Electrospinning: A fascinating fiber fabrication technique. *Journal of Biotechnology Advances*, *28*, 325–347.

Biorge, D., Dales, N., De Vrieze, S., Dejans, P., Van Camp, T., Audenaert, W., et al. (2009). Performance assessment of electrospun nanofibers for filter applications. *Journal of Desalination*, *249*, 942–948.

Celebioglu, A., Aytac, Z., Umu, O. C., Dana, A., Tekinay, T., & Uyar, T. (2014). One-step synthesis of size-tunable Ag nanoparticles incorporated in electrospun PVA/cyclodextrin nanofibers. *Journal of Carbohydrate Polymers*, *90*, 808–816.

Chen, J. W., Tseng, K. F., Delimartin, S., Lee, C. K., & Ho, M. H. (2008). Preparation of biocompatible membranes by electrospinning. *Journal of Desalination*, *233*(1–3), 48–54.

Dash, B. C., Mandal, B. B., & Kundu, S. C. (2009). Silk gland sericin protein membranes: Fabrication and characterization for potential biotechnological applications. *Journal of Biotechnology*, *144*, 321–329.

Dilamian, M., Montazer, M., & Masoumi, J. (2013). Antimicrobial electrospun membranes of chitosan/poly(ethylene oxide) incorporating poly(hexamethylene biguanide) hydrochloride. *Journal of Carbohydrate Polymers*, *94*(1), 364–371.

Doakhan, S., Montazer, M., Rashidi, A., Moniri, R., & Moghadam, M. B. (2013). Influence of sericin/TiO_2 nanocomposite on cotton fabric: Part 1. Enhanced antibacterial effect. *Journal of Carbohydrate Polymers*, *94*, 737–748.

Domard, A. (2011). A perspective on 30 years research on chitin and chitosan. *Journal of Carbohydrate Polymers*, *84*, 696–703.

Elsabee, M. Z., Naguib, H. F., & Elsayed Morsi, R. (2012). Chitosan based nanofibers, review. *Journal of Material Science and Engineering C*, *32*, 1711–1726.

Geng, X., Kwon, O.-H., & Jang, J. (2005). Electrospinning of chitosan dissolved in concentrated acetic acid solution. *Journal of Biomaterials*, *26*, 5427–5432.

Gimenes, M. L., Liu, L., & Feng, X. (2007). Sericin/poly(vinyl alcohol) blend membranes for pervaporation separation of ethanol/water mixtures. *Journal of Membrane Science*, *295*, 71–79.

Hang, Y., Zhang, Y., Jin, Y., Shao, H., & Hu, X. (2012). Preparation of regenerated silk fibroin/silk sericin fibers by coaxial electrospinning. *Journal of Biological Macromolecules*, *51*, 980–986.

Jia, Y.-T., Gong, J., Gu, X.-H., Kim, H.-Y., Dong, J., & Shen, X.-Y. (2007). Fabrication and characterization of poly (vinyl alcohol)/chitosan blend nanofibers produced by electrospinning method. *Journal of Biological Macromolecules*, *67*, 403–409.

Jin, G., Prabhakaran, M. P., Kai, D., Annamalai, S. K., Arunachalam, K. D., & Ramakrishna, S. (2013). Tissue engineered plant extracts as nanofibrous wound dressing. *Journal of Biomaterials*, *34*, 724–734.

Khajavi, R., & Abbasipour, M. (2012). Electrospinning as a versatile method for fabricating coreshell, hollow and porous nanofibers. *Journal of Scientia Iranica*, *19*(6), 2029–2034.

Kim, S. J. (2007). *Gas permeation through water-swollen sericin/PVA membranes*. Waterloo, ON, Canada.

Kundu, B., & Kundu, S. C. (2012). Silk sericin/polyacrylamide in situ forming hydrogels for dermal reconstruction. *Journal of Biomaterials*, *33*(30), 7456–7467.

Min, B. M., Lee, G., Kim, S. H., Nam, Y. S., Lee, T. S., & Park, W. H. (2004). Electrospinning of silk fibroin nanofibers and its effect on the adhesion and spreading of normal human keratinocytes and fibroblast in vitro. *Journal of Biomaterials*, *25*, 1289–1297.

Montazer, M., Shamei, A., & Alimohammadi, F. (2012). Synthesizing and stabilizing silver nanoparticles on polyamide fabric using silver-ammonia/PVP/UVC. *Journal of Organic Coatings*, *75*(4), 379–385.

Montazer, M., Alimohammadi, F., Shamei, A., & Rahimi, M. K. (2012). In situ synthesis of nano silver on cotton using Tollens' reagent. *Journal of Carbohydrate Polymers*, *87*(2), 1706–1712.

Mottaghitlab, F., Farokhi, M., Mottaghitalab, V., Ziabari, M., Divsalar, A., & Shokrgozar, M. A. (2011). Enhancement of neural cell lines proliferation using nano-structured chitosan/poly(vinyl alcohol) scaffold conjugated with nerve growth factor. *Journal of Carbohydrate Polymers*, *86*, 526–535.

Muzzarelli, R. A. A. (1985). Removal of uranium from solutions and brines by a derivative of chitosan and ascorbic acid. *Journal of Carbohydrate Polymers*, *5*(2), 85–89.

Muzzarelli, R. A. A. (2009). Chitins and chitosans for the repair of wounded skin, nerve, cartilage and bone. *Journal of Carbohydrate Polymers*, *76*(2), 167–182.

Muzzarelli, R. A. A. (2011a). Chitosan composites with inorganics, morphogenetic proteins and stem cells, for bone regeneration. *Journal of Carbohydrate Polymers*, *83*(4), 1433–1445.

Muzzarelli, R. A. A. (2011b). Potential of chitin/chitosan-bearing materials for uranium recovery: An interdisciplinary review. *Journal of Carbohydrate Polymers*, *84*(1), 54–63.

Muzzarelli, R. A. A., Weckx, M., & Filippini, O. (1989). Removal of trace metal ions from industrial waters, nuclear effluents and drinking water, with the aid of cross-linked N-carboxymethyl chitosan. *Journal of Carbohydrate Polymers*, *11*(4), 293–306.

Muzzarelli, R. A. A., Greco, F., Busilacchi, A., Sollazzo, V., & Gigante, A. (2012). Chitosan, hyaluronan and chondroitin sulfate in tissue engineering for cartilage regeneration: A review. *Journal of Carbohydrate Polymers*, *89*(3), 723–739.

Park, W. H., Jong, L., Dong, I. Y., & Hudson, S. (2004). Effect of chitosan on morphology and conformation of electrospun silk fibroin nanofibers. *Journal of Polymer*, *45*, 7151–7157.

Ramakrishna, S., Fujihara, K., Teo, W. E., Lim, T. Ch., & Ma, Z. (2005). *An introduction to electrospinning and nanofibers*. Singapore: Publishing Co.

Ravi Kumar, M. N. V. (2000). A review of chitin and chitosan applications. *Journal of Reactive & Functional Polymers*, *46*, 1–27.

Sencadas, V., Correia, D. M., Areias, A., Botelho, G., Fonseca, A. M., Neves, I. C., et al. (2012). Determination of the parameters affecting electrospun chitosan fiber size distribution and morphology. *Journal of Carbohydrate Polymers*, *87*, 1295–1301.

Sill, T. J., & Recum, H. A. (2008). Electrospinning: Applications in drug delivery and tissue engineering. *Journal of Biomaterials*, *29*, 1989–2006.

Srihanam, P., Simcheur, W., & Srisuwan, Y. (2009). Study on silk sericin and chitosan blend film: Morphology and secondary structure characterizations. *Journal of Biological Sciences*, *12*(22), 1487–1490.

Su Rho, K., Jeong, L., Lee, G., Seo, B. M., Jeon Park, Y., Hong, S. D., et al. (2006). Electrospinning of collagen nanofibers: Effects on the behavior of normal human keratinocytes and early-stage wound healing. *Journal of Biomaterials*, *27*, 1452–1461.

Terada, S., Sasaki, M., Yanagihara, K., & Yamada, H. (2005). Preparation of silk protein sericin as mitogenic factor for better mammalian cell culture. *Journal of Bioscience and Bioengineering*, *100*(6), 667–671.

Wang, Y., Zhang, Q., Zhang, Ch.-L., & Li, P. (2012). Characterisation and cooperative antimicrobial properties of chitosan/nano-ZnO composite nanofibrous membranes. *Journal of Food Chemistry*, *132*, 419–427.

Zhang, Y.-Q. (2002). Applications of natural silk protein sericin in biomaterials. *Journal of Biotechnology Advances*, *20*, 91–100.

Zhang, X., Tsukada, M., Morikawa, H., Aojima, K., Zhang, G., & Miura, M. (2011). Production of silk sericin/silk fibroin blend nanofibers. *Nanoscale Research Letters*, *6*(1), 510.

Zhang, X., Rahman Khan, Md. M., Yamamoto, T., Tsukada, M., & Morikawa, H. (2012). Fabrication of silk sericin nanofibers from a silk sericin-hope cocoon with electrospinning method. *Journal of Biological Macromolecules*, *50*, 337–347.

Zhuang, X., Cheng, B., Kang, W., & Xu, X. (2010). Electrospun chitosan/gelatin nanofibers containing silver nanoparticles. *Journal of Carbohydrate Polymers*, *82*, 524–527.